Electron transfers in proteins: Investigations with a modified through-bond coupling model

Ye-Fei Wang,[1] Gang Yang,[1,2] and Cheng-Bu Liu[1,*]
[1]*Institute of Theoretical Chemistry, Shandong University, Jinan, 250100 Shandong, People's Republic of China*
[2]*Key Laboratory of Forest Plant Ecology, Ministry of Education, Northeast Forestry University, Harbin 150040, People's Republic of China*

(Received 16 February 2009; revised manuscript received 15 July 2009; published 21 August 2009)

By integrating the merits of previous models, a modified through-bond coupling (MTBC) model is proposed in this work and shows obvious improvement compared with previous models. With the MTBC model, the dominant electron coupling pathways in the polypeptide chains were identified, where the N-H bonds were found to be essential to the electron couplings. The local structures of peptides and proteins were finely characterized by the electron couplings and decay factors since they are structure sensitive. The neighboring carbonyl O-O distances are qualitatively correlated with the decay factors, and the deviations from the transconfigurations will weaken the coupling interactions. When the two amino acids being studied are not close in sequence, the couplings through hydrogen bonds are probably the main pathway because the electron transfers in this way save many steps, albeit the decay factor is less than that of per bond, consistent with the classical electron-tunneling model developed by Beratan *et al.* [Science **252**, 1285 (1991)]. It was found that the MTBC model can be effectively extended to study the electron transfers in complex biological systems with the combination of the fragment approach, which takes into account the contributions of key hydrogen bonds.

DOI: 10.1103/PhysRevE.80.021927 PACS number(s): 87.15.A−

I. INTRODUCTION

With the exception of RNA viruses, all the organisms store their permanent information in DNA, and their gene codes are generally represented with the sequence of nucleotides. Accordingly, the intact and stable sequence of DNA is a prerequisite to reserve the life characteristics of filial generations [1]. However, the alkylation, radiation, hydrolysis, and errors during DNA replication can cause damages to the DNA structures or alterations of the DNA sequences [2–4]. The changes may increase genetic diversities, but more often leads to unwanted mutations and even diseases. Accordingly, the efficient DNA repair systems have to be developed in organisms [5,6]. Base excision repair (BER) is one of the most common repair pathways. The BER enzymes are closely involved in the removal of damaged bases, the first and crucial step of the BER processes [7–9].

As a human analog of the BER enzymes, the adenine glycosylase activity and catalytic strategies of MutY have been studied extensively [10–14]. It is hypothesized that MutY specifically recognizes 7,8-dihydro-8-oxo-2′-deoxyguanosine:2′-deoxyadenosine (OG:A) mismatches in DNA and catalyzes the hydrolysis of N-glycosidic bonds in order to remove adenine from OG:A mispairs [15–17]. The experimental results indicated that the $[Fe_4S_4]^{2+}$ cluster in MutY plays a crucial role for the adenine glycosylase activity and the binding affinity with substrates, although it does not participate in the protein folding or cause large structural alterations [12]. Based on the redox properties of the $[Fe_4S_4]^{2+/3+}$ cluster and the long-range electron transfer (ET) theory, Barton *et al.* [13,14,18,19] proposed a model to elucidate the rapid detection and reorganization of MutY during the DNA damage processes. When MutY approaches DNA, the oxidation of this protein drives ET to an alternate repair protein bound at another site, thus promoting the redistribution of MutY along the DNA duplex. Because the DNA-mediated ET process cannot proceed through the DNA damages, MutY recognizes the mismatches quickly and efficiently. In this model, the $[Fe_4S_4]^{2+/3+}$ cluster donates electrons when MutY approaches DNA, and accepts electrons when the protein dissociates from the DNA duplex. That is, the ET process will occur via two opposite directions when to bind or dissociate from DNA duplex.

In this work, the ETs in the MutY protein were investigated by a modified through-bond coupling (MTBC) model. The MTBC model integrates the merits of the Beratans' classical [20–24] and Millers' through-bond coupling models [25–27], with the details given in Sec. II A. The proposed MTBC model was first tested by performing calculations on several hydrocarbon diradicals. Besides the investigations of ETs in the polypeptide chain, the properties of the decay factors were discussed as well. Finally, the MTBC model was extended to treat the ET in complex biological systems with the combination of the fragment approach [28,29].

II. COMPUTATIONAL DETAILS

A. MTBC model

In proteins, the electronic interactions between donors and acceptors are usually rather weak [30,31]. The long-distance ET involve the electron tunneling through the peptide chains. Beratan *et al.* [20–24] developed a classical per-bond electron-tunneling model, using a basis of atoms or bonds. It thus correlated the donor-acceptor coupling and the ET rate

*Author to whom correspondence should be addressed. FAX: 0086 531 88564464; cbliu@sdu.edu.cn

$$\kappa_{\mathrm{ET}} = \frac{2\pi}{h}|T_{DA}|^2(F), \tag{1}$$

where T_{DA} and F are the electron-tunneling matrix element and Franck-Condon factor, respectively. For a single physical pathway, the electron-tunneling matrix element (t_{DA}) is defined as a collection of interacting bonds that make contributions to the donor-acceptor interactions [32,33],

$$t_{DA} = P\prod_{i=1}^{N}\varepsilon_i, \tag{2}$$

where ε_i represents the decay factor per step along the tunneling pathway. The prefactor P in Eq. (2) is dependent on the interactions between the electron donor (acceptor) with the first (last) bond of the tunneling pathway. P and F can be considered as constants for similar fragments, and accordingly the ET rates can be determined by the coupling strengths corresponding to the product terms ($\Pi\varepsilon_i$).

The classic model includes both bonding and antibonding contributions and can identify the dominant physical pathways; nonetheless, the results will be greatly influenced by the selection of semiempirical parameters. In the latter developed through-bond coupling (TBC) model [25–27,34–38], the Fock matrix elements derived from the natural bond orbitals [39–44] were used to calculate the electron couplings through the rigid organic bridges. The electron coupling elements of several hydrocarbons were calculated in this way, and the tendencies were found in reasonable agreement with the experimental data [25]. However, every coupling step of the TBC model considered either bonding or antibonding contributions instead of both as in the classic tunneling model.

To combine the merits of the above two models [45], a MTBC model was proposed in this work. In the MTBC model, the Fock matrix elements derived from the natural bond orbitals were used to calculate the electron couplings. The decay factor per step is the summation of bonding and antibonding interactions, as shown in Fig. 1, where a_1, b_1, a_2, and b_2 are the normalized coefficients of hybrid orbitals, and F_{ij} is the Fock matrix element. The idealized correlations among the different Fock matrix elements were given [22],

$$\frac{F_{ee}}{-a_1b_2} = \frac{F_{hh}}{b_1a_2} = \frac{F_{eh}}{a_1a_2} = \frac{F_{he}}{-b_1b_2} = F_{12}. \tag{3}$$

A_i was defined to be the wave-function amplitude on the ith bonding orbital and A_i^* to be the one on the corresponding antibonding orbital. Then the amplitudes on bond 2, i.e., A_2 and A_2^*, can be given as function of A_1 and A_1^* [22],

$$A_2 = \frac{F_{hh}A_1 + F_{eh}A_1^*}{E - E_b^{(2)}}, \tag{4a}$$

$$A_2^* = \frac{F_{he}A_1 + F_{ee}A_1^*}{E - E_a^{(2)}}, \tag{4b}$$

where E_a and E_b represent the antibonding and bonding orbital energies, respectively. E is the energy of tunneling electron and equals the average of the highest occupied molecular orbital (HOMO) and the lowest unoccupied molecular orbital (LUMO) energies; i.e., $(E_{\mathrm{HOMO}}+E_{\mathrm{LUMO}})/2$ [22,32]. Then, the decay factor from bond 1 to bond 2 can be written as [22]

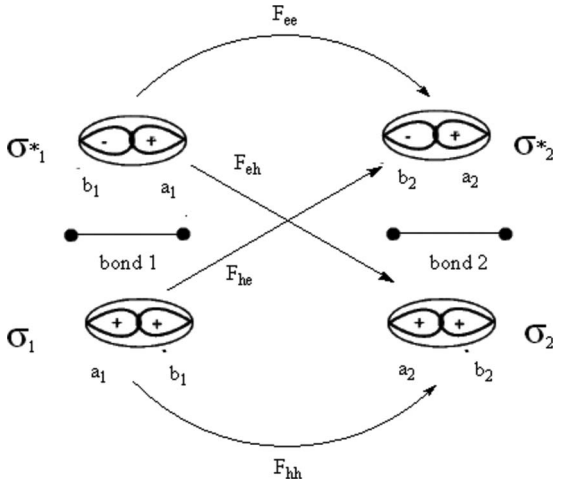

FIG. 1. The interactions between two natural bond orbitals are shown. σ and σ^* stand for the bonding and antibonding orbitals, respectively.

$$\varepsilon_2 = \frac{a_2A_2^* + b_2A_2}{b_1A_1 + a_1A_1^*} = \frac{a_2b_2F_{12}(E_b^{(2)} - E_a^{(2)})}{(E - E_b^{(2)})(E - E_a^{(2)})}. \tag{5}$$

By defining $F_{12}^{eff} = a_2b_2F_{12}$, the decay factor was divided into electron and hole contributions [22], see the equation below,

$$\varepsilon_i = \varepsilon_e + \varepsilon_h = -\frac{F_{12}^{eff}}{E - E_a^{(2)}} + \frac{F_{12}^{eff}}{E - E_b^{(2)}}. \tag{6}$$

Thus, the decay factor of the electron couplings can be obtained with the MTBC model, including both bonding and antibonding contributions for each step.

B. Computational models and methods

The crystal structure of MutY at 1.2 Å resolution was taken from Protein Date Bank (PDB code: 1KG2) [46]. As Fig. 2 indicates, MutY attacks the DNA at the Met1-Cys192 peptide chain; however, the whole peptide chain is far beyond the current *ab initio* computational methods. According to the protein pruning method [47–49], only the amino acids involved in the electron tunneling between donor and accepter contribute to the tunneling amplitude. The elimination of less important groups reduces the size of systems and thus allows for the accurate and facile descriptions of the tunneling processes. Because of the special role played by the $[Fe_4S_4]^{2+/3+}$ cluster, a polypeptide chain with six amino acid residues was truncated from this terminus; i.e., it contains Cys192, Ile191, Met190, Ala189, Gly188, and Leu187. As the positions of the heavy atoms (e.g., C, N, and O) have been precisely determined by the experimental technique, they were fixed at their experimental Cartesian coordinates in order to retain the local structures of MutY. However, the

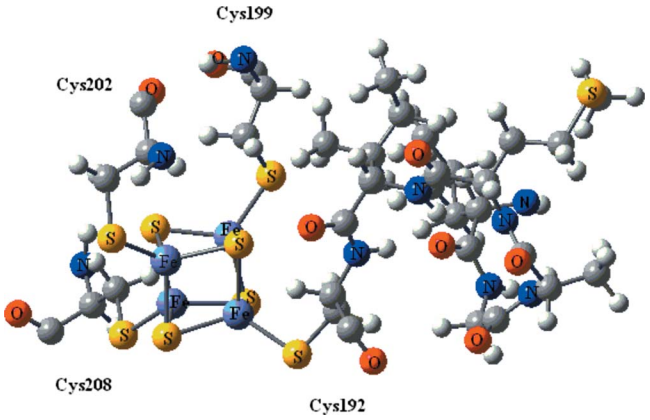

FIG. 2. (Color online) The local structure of the $[Fe_4S_4]^{2+/3+}$ cluster in the MutY protein. The truncated polypeptide chain contains Cys192, Ile191, Met190, Ala189, Gly188, and Leu187.

Cartesian coordinates of the hydrogen atoms are very difficult to be determined, and therefore the hydrogen atoms used to saturate the polypeptide chain were optimized with the B3LYP/6–31G(d) density-functional method [50–55]. The natural bond orbital (NBO) analysis was carried out at HF/6-31+G(d,p) level of theory [25–29,56–59].

The rationality of the MTBC model were first tested by the calculations on four hydrocarbon diradicals, which were previously studied by Miller *et al.* [25] at HF/3–21G level of theory. In this work, the NBO analysis of these hydrocarbon diradicals was revisited at HF/6-31+G(d,p) level, consistent with the polypeptide chain. All the calculations were run using the GAUSSIAN03 software packages [60].

III. RESULTS AND DISCUSSION

A. Testing the MTBC model

First of all, the present MTBC model was compared with the TBC model proposed by Miller *et al.* [25–27]. Four hydrocarbon diradicals with the experimental data available to us were selected as the targets. They are 1,5cD (1,5-dimethylene-*cis*-decalin), 1,5tD (1,5-dimethylene-*trans*-decalin), bcO (1,4-dimethylene-bicyclooctane), and 1,4C (1,4-dimethylene-cyclohexane), see Fig. 3.

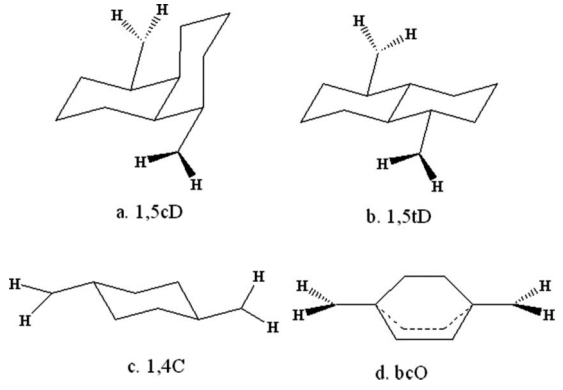

FIG. 3. Structures of 1,5cD, 1,5tD, 1,4C, and bcO (Ref. [25]).

TABLE I. The electron coupling ratios of the four hydrocarbon diradicals obtained at UHF/6-31+G(d,p) level of theory.

	Experimental[a]	$\lvert\Pi\varepsilon_i\rvert$	$\lvert V_k\rvert$	$\lvert V_{\text{chain}}\rvert$ [a,b]
1,5cD	1	1	1	1
1,5tD	1.21	1.00	0.98	0.92
1,4C	1.00	1.03	0.80	1.21
bcO	1.00	0.98	0.52	0.51

[a]Data are taken from Ref. [25].
[b]The calculated data at UHF/3–21G level of theory.

According to the TBC model, the superexchange (SE) method [61–64] was used to evaluate the electronic couplings. The elements through a coupling path (kth) between the donor and acceptor were given by

$$V_k = -\prod(-\beta_{ij})/\Pi(B_i), \tag{7}$$

where β_{ij} is the coupling between the ith and jth states, and B_i is the energy difference between the tunneling electrons and the ith state. Bi and β_{ij} were obtained from the off-diagonal and diagonal elements of the NBO Fock matrix. The total coupling is the algebraic sum over all the chains,

$$V = \sum V_k. \tag{8}$$

For the four hydrocarbon diradicals, both of the electron donors and acceptors are the methylene groups. The $\Pi\varepsilon_i$ and V_k ratios were reported in Table I together with the experimental and calculated V ones [25]. For 1,5tD and 1,4C, the V_k and V ratios of the TBC model have 20% deviations away from the experimental ones. The deviations of bcO are even larger and approximate 50%. As discussed by Miller *et al.* [25], the calculated and experimental inconsistencies were probably due to the uncertainty of the theoretical couplings because of dependence of the geometries and the use of methylene groups in place of the larger chromophores. The present MTBC model considers the contributions of both bonding and antibonding per step. The deviations of the ratios are equal to 2% for bcO, 3% for 1,4C, and 17% for 1,5tD, respectively (Table I). Accordingly, the MTBC model is qualitatively improved when compared with the TBC model. It urges us to study the ETs in biological systems with the MTBC model.

B. Identifying the dominant electron coupling pathways

As described in Sec. II A, the ET rates in the polypeptide chains are expected to be dominated by the main coupling pathways since the contained amino acid residues have very close P and F factors. The identifications of the main electron coupling pathways are in fact to maximize the $\Pi\varepsilon_i$ products in Eq. (2).

Compared with the classical electron-tunneling model, there are two obvious improvements in the present MTBC model. First, all the ε_i values were calculated without any semiempirical parameter. For typical σ bonds, the decay of wave function (ε_i) occurs either through the direct bonds or through space. In the classic model, the semiempirical pa-

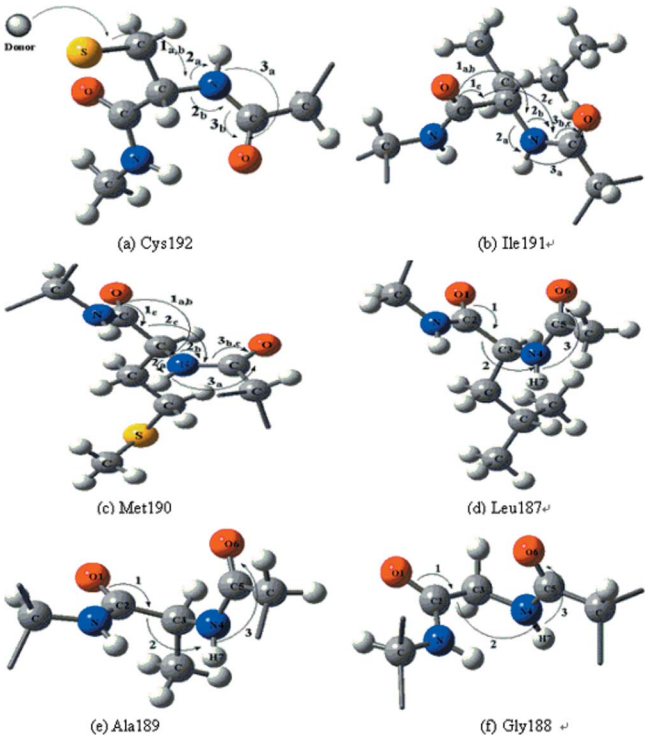

FIG. 4. (Color online) The possible coupling pathways of the Cys192, Ile191, Met190, Ala189, Gly188, and Leu187 subgroups. The Arabic numbers represent the coupling steps while a, b, or c indicates different pathways.

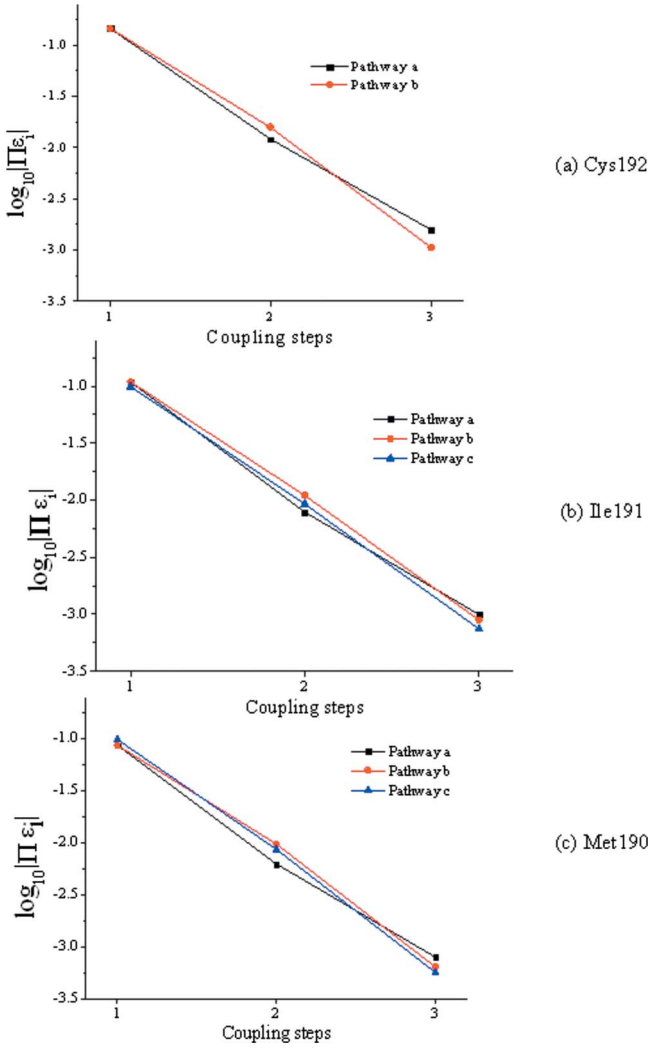

FIG. 5. (Color online) The decay curves of possible coupling pathways through the Cys192, Ile191, and Met190 subgroups.

rameters derived from experiments were introduced to estimate the decay factors [20], and as a natural result their values will be seriously influenced by the selection of semiempirical parameters [65]. In addition, the use of semiempirical parameters in the classical model neglects structural fluctuations. The recent studies [66–68] pointed out that structural fluctuations play an important role in the electron couplings of peptide chains. The above deficiencies can be reduced a lot with the present MTBC model because no semiempirical parameters are used. In the MTBC model, the Fock matrix elements were derived directly from *ab initio* computations. Accordingly, the coupling elements are sensitive to chemical environments and will correctly reflect the local structures of the investigated systems. Second, the MTBC model reduces greatly the number of decay steps compared with the classical per-bond strategy. The ε_i values per step range from 0.08 to 0.15. It is important to note that one decay step in the MTBC model approximates two per-bond steps. Therefore, the decay factor per bond (ε) is about 0.28–0.39, somewhat lower than the experimental data (0.4–0.6) [21,22,32,33]. It was probably caused by the neglect of minor coupling pathways. The decay of the dominant pathway is lower than that of all the possible pathways [Eq. (8)].

The polypeptide chain in Fig. 2 consists of six amino acids; namely, Cys192, Ile191, Met190, Ala189, Gly188, and Leu187. The possible electron coupling pathways through the direct bonds were shown in Fig. 4, where the various coupling pathways were distinguished by a, b, c, etc. The coupling steps of each pathway were labeled by the Arabic numerals. Take Cys192 in Fig. 4(a) for example. There are two possible coupling pathways, i.e., Pathway a and Pathway b. For Pathway a, three coupling steps are involved and numbered as 1 (from S-C bond to C-N bond), 2 (from C-N bond to N-H bond), and 3 (from N-H bond to C=O bond), respectively. The decay curves were shown in Fig. 5. Owing to the larger $\Pi\varepsilon_i$ value, Pathway a rather than Pathway b plays a dominant role in the case of Cys192. Ile191 and Met190 each have three possible coupling pathways, and their roles increase in the same orders of Pathway b < Pathway c < Pathway a. After analysis it was found that all the dominant coupling pathways in Cys192, Ile191, and Met190 contain the N-H bonds. As Figs. 4(d)–4(f) indicated, only one coupling pathway exists for Ala189, Gly188, or Leu187. Interestingly, the N-H bonds are also involved in the coupling pathways of Ala189, Gly188, or Leu187. Accordingly, the N-H bonds are essential to the electron couplings in biological systems.

For the amino acid residues in peptides and proteins which are not close in sequence, the electron couplings through direct bonds may undergo numerous bonds whereas through hydrogen bonds will save many steps. For the N-H $\rightarrow$O=C segment, the $|\varepsilon_i|$ value was calculated to be 0.039

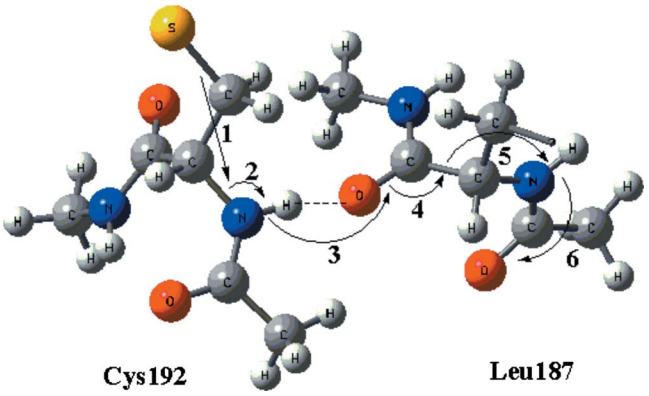

FIG. 6. (Color online) The coupling pathway through the hydrogen bond formed between Cys192 and Leu187.

for couplings directly through the N-H→O=C hydrogen bond approximates; one-third of that through the covalent bond. The electron couplings of the chosen polypeptide chains through hydrogen bond were shown in Fig. 6. It was found that the couplings through hydrogen bond save 12 steps altogether, causing the $|\varepsilon_i|$ value 10^{12} larger than that through covalent bond according to Eq. (2). The electron couplings are of 10^{-5} and 10^{-17} orders through hydrogen bond and covalent bond, respectively. It is consistent with the findings of Beratan *et al.* [22,23]. They used the classical electron-tunneling model on the native protein systems and found that the rate of long-range electron transfers decreases rapidly with the distance and the couplings through hydrogen bonds obviously shorten the distance. Note that the decay step through hydrogen bond in the MTBC model is also equal to two per-bond steps, the same as that through covalent bond. For example, the decay step of the N-H→O=C hydrogen bond in the MTBC model occurs directly from N-H to C=O, which amount to two per-bond steps, i.e., from N-H to H···O and then from H···O to C=O. In the classical electron-tunneling model, the decay factor through hydrogen bond (ε_H) approximates the squared value of covalent bond (ε_B) [20,65], in reasonable agreement with the experimental data [69–74]. Accordingly, the couplings through hydrogen bond in the MTBC model are expected to be about ε_B^3 [75]. The $|\varepsilon_i|$ value through N-H→O=C hydrogen bond obtained by the present MTBC model is close to that reported by Cave *et al.* [76].

C. Properties of the decay factor

As shown in Fig. 4, the electron coupling pathways through the polypeptide chains are closely correlated with the orientations of the carbonyl groups. It is assumed that the interactions among the neighboring carbonyl groups exert a large influence on the decay factors [77–83]. The O-O distances of the neighboring carbonyl groups and the decay factors were plotted in Fig. 7. Note that the amino acid codes of the abscissa in Fig. 7 correspond to the fragments of Fig. 4. The O-O distances and decay factors were found to change contrarily to each other. In other words, the decay factors are sensitive enough to the carbonyl O-O distances

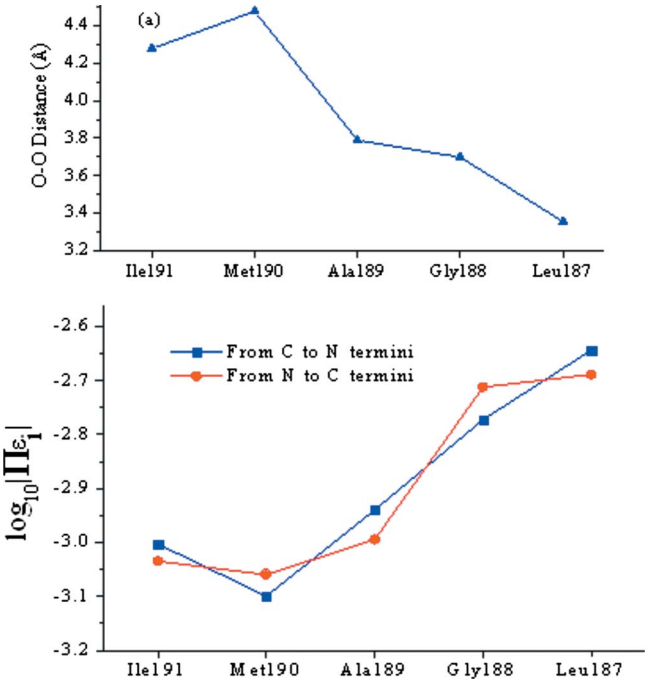

FIG. 7. (Color online) The neighboring carbonyl O-O distances (a) and decay factors via two opposite directions (b) for the subgroups in Fig. 4.

and increase with the decrease in the carbonyl O-O distances [83].

As the previous literatures indicated [84,85], Ala and Gly quite resemble each other and therefore Ala189 and Gly188 were used to clarify the chemical sensitivity of the decay factors. It was found from Figs. 4(e) and 4(f) that the coupling steps of Ala189 and Gly188 are exactly identical, confirming the resemblances of these two amino acids. However, obvious differences were observed between their electron couplings, especially in Step 2 involving the N-H bonds, see Fig. 8. The $\psi(C_2C_3N_4H_7)$ and $\psi(H_7N_4C_5O_6)$ dihedrals were optimized at 87.54° and −168.68° in Ala189 [Fig. 4(e)] and 112.53° and 176.95° in Gly188 [Fig. 4(f)],

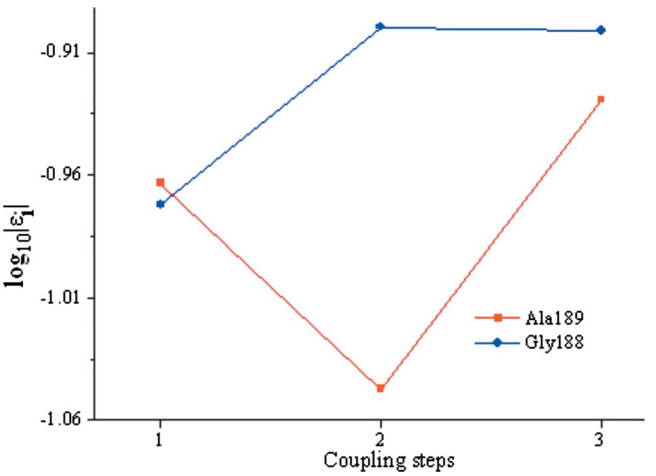

FIG. 8. (Color online) The per-step decay factors of the Ala189 and Gly188 subgroups.

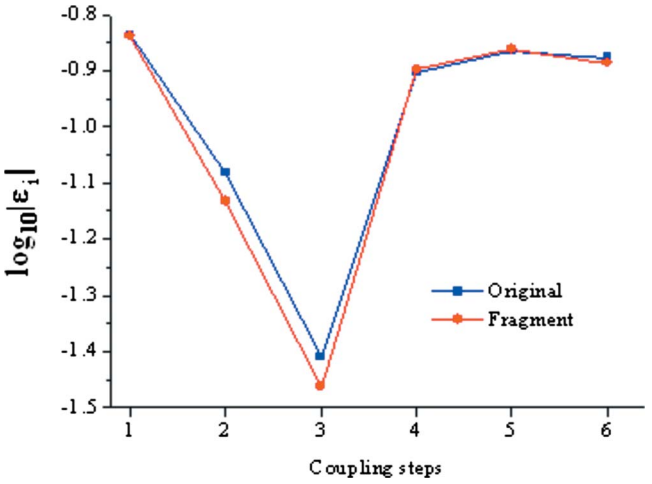

FIG. 9. (Color online) The decay factors from Cys192 to Leu187 obtained by the original and fragment approaches.

respectively. The absolute values ($|\psi|$) of the Gly188 dihedrals are larger than the corresponding ones of Ala189 and as a result will have larger decay factors. Hoffmann and his co-workers [86,87] once observed that all the trans-isomers have the largest through-bond interactions and the deviations will weaken the interactions, in excellent agreement with the present results obtained by the MTBC model.

As indicated in Sec. I, the ET processes will occur in two opposite directions. This assumption was validated by the decay factors plotted in Fig. 7. The decay factors in each direction increase with the decrease in the carbonyl O-O distances and also sensitive to the dihedrals, which are identical to the total decay factors as discussed above.

D. Combination of the fragment approach

As is well known to us, it is beyond the current computing powers to run *ab initio* calculations on large biological systems such as proteins. For this purpose, the fragment approach was attempted, combining with the presently proposed MTBC model. The discussions in Sec. III B indicated in the polypeptide chains, the decay through hydrogen bonds formed between Cys192 and Leu187, is the dominant coupling pathway. To the best of our knowledge, the hydrogen bond networks are universal in all the complex biological systems. The fragment approach will greatly simplify the systems by neglecting the subgroups that are not involved in the key hydrogen bonds. Take the present polypeptide chains for example. The fragment approach does not take into account the roles of the Ile191, Met190, Ala189, and Gly188 (Fig. 5). In this way, the decay factors were calculated and shown in Fig. 9, together with those of the original approach taking into calculations of all the amino acid residues. It was found that the decay curves of these two approaches suit perfectly with each other. Accordingly, the MTBC model can be effectively extended to deal with the ETs in much more complex biological systems by combining with the fragment approach.

IV. CONCLUSIONS

In this work, a modified through-bond coupling (MTBC) model was proposed to study the electron transfers (ET) in biological systems, by integrating the merits of the previous Beratans' classical and Millers' through-bond coupling models. The further combination with the fragment approach shows great potentials to study the ET in complex biological systems.

Several hydrocarbon diradicals were chosen to test the proposed MTBC model. It was found that the MTBC model shows obvious improvement and thus better agreement with the experimental results when compared with the previous models. In the MTBC model, the Fock matrix elements were derived directly from *ab initio* computations and no semiempirical parameters were used; in addition, every coupling step considers both bonding and antibonding contributions.

The electron couplings in the polypeptide chains were investigated by the MTBC model. The dominant coupling pathways were identified by maximizing the product terms ($\Pi\varepsilon_i$) in Eq. (2). It was found that the N-H bonds are essential to the electron couplings in biomolecules such as peptides and proteins. The coupling pathways involving the N-H bonds play a dominant role. In addition, for two segregated amino acid residues, the couplings through the hydrogen bonds are probably the dominant pathways by saving many steps. For example, the electron couplings between Cys192 and Leu187 through the hydrogen bond and direct bonds are of 10^{-5} and 10^{-17} orders, respectively.

According to the MTBC model, the electron couplings and decay factors are sensitive to the chemical environments, thus correctly characterizing the local structures of the peptides and proteins. It was found the decay factors increase with the decrease in the neighboring carbonyl O-O distances. The deviations from the transconfigurations will weaken the couplings. The couplings were found to occur via two opposite directions.

As hydrogen bonds are ubiquitous in biomolecules, it is suggested to adopt the fragment approach by considering the contributions of only the key hydrogen bonds. The results showed that with combination of the fragment approach, the MTBC model can be effectively extended to deal with the electron transfers in complex biological systems.

ACKNOWLEDGMENTS

This work is supported by the National Natural Science Foundations of China (Grants No. 20633060 and No. 20873075), and by the Major State Basic Research Development Programs (Grant No. 2004CB719902).

[1] M. K. Shigenaga and B. N. Ames, Free Radic Biol. Med. **10**, 211 (1991).
[2] T. Lindahl, Nature (London) **362**, 709 (1993).
[3] M. Berwick and P. Vineis, J. Natl. Cancer Inst. **92**, 874 (2000).
[4] B.-B. S. Zhou and S. J. Elledge, Nature (London) **408**, 433 (2000).
[5] G. I. Evan and K. H. Vousden, Nature (London) **411**, 342 (2001).
[6] M. Takata, M. S. Sasaki1, E. Sonoda, C. Morrison, M. Hashimoto, H. Utsumi, Y. Yamaguchi-Iwai, A. Shinohara, and S. Takeda, EMBO J. **17**, 5497 (1998).
[7] H. E. Krokan, R. Standal, and G. Slupphaug, Biochem. J. **325**, 1 (1997).
[8] O. D. Scharer, Angew. Chem. Int. Ed. Engl. **42**, 2946 (2003).
[9] S. S. David and S. D. Williams, Chem. Rev. **98**, 1221 (1998).
[10] A. W. Francis, S. A. Helquist, E. T. Kool, and S. S. David, J. Am. Chem. Soc. **125**, 16235 (2003).
[11] P. J. Berti and J. A. B. McCann, Chem. Rev. **106**, 506 (2006).
[12] S. L. Porello, M. J. Cannon, and S. S. David, Biochemistry **37**, 6465 (1998).
[13] E. Yavin, A. K. Boal, E. D. A. Stemp, E. M. Boon, A. L. Livingston, V. L. O'Shea, S. S. David, and J. K. Barton, Proc. Natl. Acad. Sci. U.S.A. **102**, 3546 (2005).
[14] A. K. Boal, E. Yavin, O. A. Lukianova, V. L. O'Shea, S. S. David, and J. K. Barton, Biochemistry **44**, 8397 (2005).
[15] M. L. Michaels, J. Tchou, A. P. Grollman, and J. H. Miller, Biochemistry **31**, 10964 (1992).
[16] S. Shibutani, M. Takeshita, and A. P. Grollman, Nature (London) **349**, 431 (1991).
[17] A. Gogos, J. Cillo, N. D. Clarke, and A. L. Lu, Biochemistry **35**, 16665 (1996).
[18] A. A. Gorodetsky, A. K. Boal, and J. K. Barton, J. Am. Chem. Soc. **128**, 12082 (2006).
[19] E. Yavin, E. D. A. Stemp, V. L. O'Shea, S. S. David, and J. K. Barton, Proc. Natl. Acad. Sci. U.S.A. **103**, 3610 (2006).
[20] D. N. Beratan, J. N. Onuchic, J. N. Betts, B. E. Bowler, and H. B. Gray, J. Am. Chem. Soc. **112**, 7915 (1990).
[21] D. N. Beratan, J. N. Onuchic, and J. J. Hopfield, J. Chem. Phys. **86**, 4488 (1987).
[22] J. N. Onuchic and D. N. Beratan, J. Chem. Phys. **92**, 722 (1990).
[23] D. N. Beratan, J. N. Betts, and J. N. Onuchic, Science **252**, 1285 (1991).
[24] J. N. Onuchic, D. N. Beratan, and J. J. Hopfield, J. Phys. Chem. **90**, 3707 (1986).
[25] B. P. Paulson, L. A. Curtiss, B. Bal, G. L. Closs, and J. R. Miller, J. Am. Chem. Soc. **118**, 378 (1996).
[26] C. A. Naleway, L. A. Curtiss, and J. R. Miller, J. Phys. Chem. **95**, 8434 (1991).
[27] L. A. Curtiss, C. A. Naleway, and J. R. Miller, J. Phys. Chem. **99**, 1182 (1995).
[28] T. R. Prytkova, I. V. Kurnikov, and D. N. Beratan, J. Phys. Chem. B **109**, 1618 (2005).
[29] I. V. Kurnikov and D. N. Beratan, J. Chem. Phys. **105**, 9561 (1996).
[30] S. Larsson, J. Am. Chem. Soc. **103**, 4034 (1981).
[31] D. N. Beratan and J. J. Hopfield, J. Am. Chem. Soc. **106**, 1584 (1984).
[32] J. N. Onuchic and D. N. Beratan, J. Am. Chem. Soc. **109**, 6771 (1987).
[33] D. N. Beratan, J. Am. Chem. Soc. **108**, 4321 (1986).
[34] M. N. Paddon-Row, S. S. Wong, and K. D. Jordan, J. Am. Chem. Soc. **112**, 1710 (1990).
[35] K. D. Jordan and M. N. Paddon-Row, Chem. Rev. **92**, 395 (1992).
[36] M. N. Paddon-Row, M. J. Shephard, and K. D. Jordan, J. Am. Chem. Soc. **115**, 3312 (1993).
[37] M. N. Paddon-Row and K. D. Jordan, J. Am. Chem. Soc. **115**, 2952 (1993).
[38] M. J. Shephard, M. N. Paddon-Row, and K. D. Jordan, J. Am. Chem. Soc. **116**, 5328 (1994).
[39] J. P. Foster and F. Weinhold, J. Am. Chem. Soc. **102**, 7211 (1980).
[40] A. E. Reed and F. Weinhold, J. Chem. Phys. **78**, 4066 (1983).
[41] A. E. Reed, R. B. Weinstock, and F. Weinhold, J. Chem. Phys. **83**, 735 (1985).
[42] F. Weinhold and T. K. Brunck, J. Am. Chem. Soc. **98**, 3745 (1976).
[43] T. K. Brunck and F. Weinhold, J. Am. Chem. Soc. **98**, 4392 (1976).
[44] A. E. Reed, L. A. Curtis, and F. A. Weinhold, Chem. Rev. **88**, 899 (1988).
[45] B. P. Paulson, J. R. Miller, W. X. Gan, and G. Closs, J. Am. Chem. Soc. **127**, 4860 (2005).
[46] R. Gilboa, A. Kilshtein, D. O. Zharkov, J. H. Kycia, S. E. Gerchman, A. P. Grollman, and G. Shoham (unpublished).
[47] P. Siddarth and R. A. Marcus, J. Phys. Chem. **94**, 2985 (1990); **97**, 2400 (1993).
[48] I. Daizadeh, J. N. Gehlen, and A. A. Stuchebrukhov, J. Chem. Phys. **106**, 5658 (1997).
[49] S. S. Skourtis, J. J. Regan, and J. N. Onuchic, J. Phys. Chem. **98**, 3379 (1994).
[50] J. R. Pliego, W. B. De Almeida, S. Celebi, Z. D. Zhu, and M. S. Platz, J. Phys. Chem. A **103**, 7481 (1999).
[51] A. D. Becke, Phys. Rev. A **38**, 3098 (1988).
[52] A. D. Becke, J. Chem. Phys. **98**, 5648 (1993).
[53] C. Lee, W. T. Yang, and R. G. Parr, Phys. Rev. B **37**, 785 (1988).
[54] A. G. Baboul, L. A. Curtiss, P. C. Redfern, and K. Raghavachari, J. Chem. Phys. **110**, 7650 (1999).
[55] L. A. Curtiss and J. R. Miller, J. Phys. Chem. A **102**, 160 (1998).
[56] R. Improta, S. Antonello, F. Formaggio, F. Maran, N. Rega, and V. Barone, J. Phys. Chem. B **109**, 1023 (2005).
[57] L. Y. Zhang, R. A. Friesner, and R. B. Murphy, J. Chem. Phys. **107**, 450 (1997).
[58] C. Kobayashi, K. Baldridge, and J. N. Onuchic, J. Chem. Phys. **119**, 3550 (2003).
[59] J. Kim and A. A. Stuchebrukhov, J. Phys. Chem. B **104**, 8606 (2000).
[60] M. J. Frisch, G. W. Trucks, H. B. Schlegel, G. E. Scuseria, M. A. Robb, J. R. Cheeseman, J. A. Montgomery, T. Vreven, K. N. Kudin, J. C. Burant, J. M. Millam, S. S. Iyengar, J. Tomasi, V. Barone, B. Mennucci, M. Cossi, G. Scalmani, N. Rega, G. A. Petersson, H. Nakatsuji, M. Hada, M. Ehara, K. Toyota, R. Fukuda, J. Hasegawa, M. Ishida, T. Nakajima, Y. Honda, O. Kitao, H. Nakai, M. Klene, X. Li, J. E. Knox, H. P. Hratchian, J. B. Cross, C. Adamo, J. Jaramillo, R. Gomperts, R. E. Stratmann, O. Yazyev, A. J. Austin, R. Cammi, C. Pomelli, J. W. Ochterski, P. Y. Ayala, K. Morokuma, G. A. Voth, P. Salvador,

J. J. Dannenberg, V. G. Zakrzewski, S. Dapprich, A. D. Daniels, M. C. Strain, O. Farkas, D. K. Malick, A. D. Rabuck, K. Raghavachari, J. B. Foresman, J. V. Ortiz, Q. Cui, A. G. Baboul, S. Clifford, J. Cioslowski, B. B. Stefanov, G. Liu, A. Liashenko, P. Piskorz, I. Komaromi, R. L. Martin, D. J. Fox, T. Keith, M. A. Al-Laham, C. Y. Peng, A. Nanayakkara, M. Challacombe, P. M. W. Gill, B. Johnson, W. Chen, M. W. Wong, C. Gonzalez, and J. A. Pople, GAUSSIAN 03, Revision B.05, Gaussian, Pittsburgh, PA, 2003.

[61] P. W. Anderson, Phys. Rev. **79**, 350 (1950).

[62] J. Halpern and L. Orgel, Discuss. Faraday Soc. **29**, 32 (1960).

[63] H. M. McConnell, J. Chem. Phys. **35**, 508 (1961).

[64] N. J. Turro and J. K. Barton, J. Biol. Inorg. Chem. **3**, 201 (1998).

[65] M. L. Jones, I. V. Kurnikov, and D. N. Beratan, J. Phys. Chem. A **106**, 2002 (2002).

[66] J. Wolfgang, S. M. Risser, S. Priyadarshy, and D. N. Beratan, J. Phys. Chem. B **101**, 2986 (1997).

[67] T. R. Prytkova, I. V. Kurnikov, and D. N. Beratan, Science **315**, 622 (2007).

[68] I. A. Balabin, D. N. Beratan, and S. S. Skourtis, Phys. Rev. Lett. **101**, 158102 (2008).

[69] P. J. de Rege, S. A. Williams, and M. J. Therien, Science **269**, 1409 (1995).

[70] C. Turro, C. K. Chang, G. E. Leroi, R. I. Cukier, and D. G. Nocera, J. Am. Chem. Soc. **114**, 4013 (1992).

[71] J. M. Hodgkiss, N. H. Damrauer, S. Pressé, J. Rosenthal, and D. G. Nocera, J. Phys. Chem. B **110**, 18853 (2006).

[72] E. R. Young, J. Rosenthal, J. M. Hodgkiss, and D. G. Nocera, J. Am. Chem. Soc. **131**, 7678 (2009).

[73] J. L. Sessler, B. Wang, and A. Harriman, J. Am. Chem. Soc. **115**, 10418 (1993).

[74] A. Harriman, Y. Kubo, and J. L. Sessler, J. Am. Chem. Soc. **114**, 388 (1992).

[75] E. Cukier and R. J. Cave, Chem. Phys. Lett. **402**, 186 (2005).

[76] W. Kurlancheek and R. J. Cave, J. Phys. Chem. A **110**, 14018 (2006).

[77] E. W. Schlag, S. Y. Sheu, D. Y. Yang, H. L. Selzle, and S. H. Lin, J. Phys. Chem. B **104**, 7790 (2000).

[78] S. Y. Sheu, D. Y. Yang, H. L. Selzle, and E. W. Schlag, J. Phys. Chem. A **106**, 9390 (2002).

[79] L. Lehr, T. Horneff, R. Weinkauf, and E. W. Schlag, J. Phys. Chem. A **109**, 8074 (2005).

[80] S. Y. Sheu, E. W. Schlag, D. Y. Yang, and H. L. Selzle, J. Phys. Chem. A **105**, 6353 (2001).

[81] P. Kulhanek, E. W. Schlag, and J. Koca, J. Am. Chem. Soc. **125**, 13678 (2003).

[82] R. Weinkauf, P. Schanen, A. Metsala, M. Bürgle, H. Kessler, and E. W. Schlag, J. Phys. Chem. **100**, 18567 (1996).

[83] E. W. Schlag, S. Y. Sheu, D. Y. Yang, H. L. Selzle, and S. H. Lin, Angew. Chem. Int. Ed. **46**, 3196 (2007).

[84] A. G. Császár, J. Phys. Chem. **100**, 3541 (1996).

[85] G. Yang, Y. G. Zu, Y. J. Fu, L. J. Zhou, R. X. Zhu, and C. B. Liu, J. Mol. Struct.: THEOCHEM **901**, 81 (2009).

[86] R. Hoffmann, A. Imamura, and W. J. Hehre, J. Am. Chem. Soc. **90**, 1499 (1968).

[87] R. Hoffmann, Acc. Chem. Res. **4**, 1 (1971).